JOURNAL OF VIROLOGY, Oct. 2000, p. 9267–9280 Vol. 74, No. 19
0022-538X/00/$04.00+0

Chemokine Gene Expression in Astrocytes of Borna Disease Virus-Infected Rats and Mice in the Absence of Inflammation

CHRISTIAN SAUDER,[1] WIEBKE HALLENSLEBEN,[1] AXEL PAGENSTECHER,[2] STEFANIE SCHNECKENBURGER,[1] LASZLO BIRO,[1] DORIS PERTLIK,[3] JÜRGEN HAUSMANN,[1] MARK SUTER,[3] AND PETER STAEHELI[1]*

Abteilung Virologie, Institut für Medizinische Mikrobiologie und Hygiene, Universität Freiburg, D-79104 Freiburg,[1] and Abteilung Neuropathologie, Universität Freiburg, D-79106 Freiburg,[2] Germany, and Institut für Virologie, Universität Zürich, CH-8057 Zürich, Switzerland[3]

Received 4 February 2000/Accepted 28 June 2000

Borna disease virus (BDV) causes $CD8^+$ T-cell-mediated meningoencephalitis in immunocompetent mice and rats, thus providing a valuable animal model for studying the mechanisms of virus-induced central nervous system (CNS) immunopathology. Chemokine-mediated leukocyte recruitment to the CNS is a crucial step in the development of neurological disease. We found increased mRNA levels of IP-10 and other chemokines in brains of adult rats following infection with BDV. The marked increase in chemokine gene expression at about day 8 postinfection seemed to immediately precede the inflammatory process. In brains of rats infected as newborns, in which inflammation was only mild and transient, sustained expression of IP-10 and RANTES genes was observed. In situ hybridization studies revealed that astrocytes were the major source of IP-10 mRNAs in brains of rats infected as newborns and as adults. In brains of infected mice lacking $CD8^+$ T cells ($\beta2m^{0/0}$), transcripts encoding IP-10 and RANTES were also observed. IP-10 transcripts were also present in a small number of scattered astrocytes of infected knockout mice lacking mature B and T cells as well as functional alpha/beta and gamma interferon receptors, indicating that BDV can induce chemokine synthesis in the absence of interferons and other B- or T-cell-derived cytokines. These data provide strong evidence that CNS-resident cells are involved in the early localized host immune response to infection with BDV and support the concept that chemokines are pivotal for the initiation of virus-induced CNS inflammation.

Viral infections of the central nervous system (CNS) may evoke robust immune responses, leading to encephalitis and tissue damage (see reference 10 for a review). In the case of viruses that affect CNS cell integrity and function, this immune response can be beneficial in limiting the spread of the virus and in restricting virus-induced CNS damage. However, some viruses infect the CNS without impairing vital cellular functions (19, 47). Immune responses following CNS infection by these noncytopathic viruses then may cause severe CNS tissue destruction, which can be more detrimental to the host than the initial viral insult.

Borna disease (BD) virus (BDV) falls into this second category of infectious agents. It is a neurotropic nonsegmented negative-stranded RNA virus that primarily infects horses and sheep. In these animals, it can cause BD, an often lethal meningoencephalitis (see reference 66 for a review). Persistent BDV infections can be established experimentally in many vertebrate species, with considerable variation in clinical outcome (see reference 30 for a review). BDV-induced disease in rats and mice has been recognized to be mediated by the immune system, with cytotoxic $CD8^+$ T cells being the major effectors (35, 73). Intracerebral infection of adult rats induces severe meningoencephalitis within 2 to 3 weeks postinfection (p.i.), manifesting itself in behavioral abnormalities and movement disorders. Likewise, following neonatal infection of disease-susceptible MRL mice, meningoencephalitis accompanied by clinical symptoms that are similar to those observed in diseased rats develops (33). In contrast, infection of newborn rats (13) leads to immunological tolerance and viral persistence in the absence of gross inflammation and disease. Similarly, mutant mice lacking $CD8^+$ T cells ($\beta2m^{0/0}$) are resistant to BDV-induced neurological disease (33).

Although it has become clear that leukocyte entry into the CNS is a crucial event in the pathogenesis of immune system-mediated CNS diseases, the exact underlying mechanisms are still not fully understood (39). Chemokines, together with proinflammatory cytokines, have been proposed to play a decisive role in leukocyte attachment to the blood-brain barrier endothelium. Furthermore, chemokines have been recognized as the key mediators of cerebral leukocyte extravasation and accumulation (3, 28, 64). Chemokines are low-molecular-weight chemoattractant peptides that are divided into four subfamilies, termed CXC (α), CC (β), C (γ), and CX_3C (δ), primarily based on the position of the first two N-terminal conserved cysteine residues but also based on functional and genetic similarities (5, 6, 55, 65). Many α-chemokines mainly act on neutrophils, whereas others, such as interferon-inducible 10-kDa protein IP-10, act on T cells. Most β-chemokines, such as MIP-1β and MCP-1, primarily attract monocytes. Some others, however, such as RANTES, also attract T cells. The action of lymphotactin, the only γ-chemokine described so far, is restricted to lymphoid cells (36). Neurotactin, representing the δ-chemokine family, seems to be involved in both leukocyte adhesion and attraction of lymphocytes, monocytes, and microglia (8, 56).

Whereas much is known about the expression of proinflammatory cytokines in the BDV-infected CNS (34, 57, 69, 71), to date only very limited data have been available concerning the role of chemokines in this viral infection. We show here that IP-10 and RANTES are strongly expressed in the brains of BDV-infected rats and mice, irrespective of whether immune

* Corresponding author. Mailing address: Department of Virology, University of Freiburg, Hermann-Herder-Str. 11, D-79104 Freiburg, Germany. Phone: 49-761-203-6579. Fax: 49-761-203-6562. E-mail: staeheli@ukl.uni-freiburg.de.

TABLE 1. Specifications of plasmids used for RPA and ISH studies

Gene	Subcloned sequence (position in gene)	Length (bp)	Vector	Polymerase and restriction enzyme used for antisense (sense) transcript	GenBank accession no.	Source or reference
Lymphotactin	20–240	221	pGEM-3Z	T7, *Hin*dIII	U23377	M. L. Jones (unpublished data)
MIP-1β	26–220[a]	195	pGEM-3Z	T7, *Hin*dIII	U06434	Jones, unpublished
	90–274	185		T7, *Hin*dIII		
RANTES	73–238	166	pGEM-3Z	T7, *Hin*dIII	U06436	Jones, unpublished
MCP-1	134–279	146	pGEM-3Z	T7, *Hin*dIII	M57441	79
Mob-1/IP-10	243–372 (RPA)	130	pGEM-3Z	T7, *Hin*dIII	U22520	77
	89–553 (ISH)	464	pGEM-3Z	T7, *Hin*dIII (SP6, *Eco*RI)		
Crg-2/IP-10[b]	34–399 (ISH)	355	pBS-KS	T7, *Eco*RI (T3, *Xba*I)	M86829	75
T3δ	75–310	236	pBS-SK(−)	T7, *Eco*RI	X53430	18, 69
T3δ[b]	299–339, 12–230, and 675–727	342	pGEM-3Z	T7, *Hin*dIII	M12728 and M12729	74
BDV p40	714–869	155	pGEM-4Z	T7, *Eco*RI	L27077	17
pMulL-1β[b]	255–397	143	pGEM-4Z	T7, *Eco*RI	M15131	40
pMuTNFα[b]	450–753	304	pGEM-4Z	T7, *Eco*RI	M11731	40
L32[b]	1219–1293 and 1931–1954	99	pGEM-3Z	T7, *Hin*dIII	K02060	21

[a] The plasmid representing this sequence was used for RPA analysis of chemokine expression in PTI-NB rat brains. For all other RPAs, a plasmid representing the region from positions 90 to 274 was used.
[b] Mouse genes. T3δ, gene encoding the delta chain of the T-cell receptor–CD3 complex. L32, gene encoding ribosomal protein L32.

cells are present or not. Furthermore, we identify astrocytes as the major source of IP-10 in these brains.

MATERIALS AND METHODS

Animals. Lewis rats were purchased from Charles River, Sulzfeld, Germany. Wild-type and $\beta 2m^{0/0}$ MRL mice were bred in our local animal facility (33). They were originally purchased from The Jackson Laboratory, Bar Harbor, Maine. Rag-$2^{0/0}$ mice lacking functional receptors for alpha/beta interferon (IFN-α/β) and IFN-γ (AGR mice) (44) were bred in the animal facility of the University of Zürich.

Virus stocks. The BDV stock used for infection of adult rats was the fourth brain passage (BDVRp4) in adult rats of the Giessen strain of He/80 of BDV. BDVRp4 (kindly provided by O. Planz and L. Stitz, Tübingen, Germany) was prepared from rat brains at 4 weeks p.i. The infectious titer (3×10^6 focus-forming units per ml) of a 10% brain homogenate was determined by an immunofocus assay (37) using Vero cells. The BDV stock used for infection of newborn rats and of adult rats euthanized at day 33 p.i. has been described elsewhere (69). Newborn mice were infected with the fifth brain passage in newborn rats of the Giessen strain of He/80 of BDV (33). Adult mice were infected with a mouse-adapted strain of BDV that was generated by passaging the rat-adapted Giessen strain of He/80 four times in brains of newborn mice and two times in brains of 4-week-old MRL mice.

Infection of rats and mice. Male Lewis rats were infected at the age of 4 to 6 weeks by injection into the left brain hemisphere of either 50 μl of BDVRp4 (1.5×10^4 focus-forming units), diluted in Dulbecco modified Eagle medium containing 2% fetal bovine serum, or 50 μl of virus diluent alone (mock infections). Rats were infected under anesthesia using methoxyflurane (Metofane; Janssen-Cilag, Neuss, Germany). Infection of newborn rats was done as described previously (69). Intracerebral infections of mice were performed by injecting 10-μl samples of undiluted virus stocks into the left brain hemisphere using a Hamilton syringe. Infections of adult mice were performed under light ether anesthesia.

Preparation of tissues for histological analysis and in situ hybridization (ISH). Rats infected as adults were euthanized with CO_2 at different time points p.i., and the brains were divided along the midline upon removal. The right brain hemispheres were dissected into the cerebellum and cerebrum, and the tissue samples were individually frozen in liquid nitrogen and stored at −70°C until RNA was prepared. The left brain hemispheres either were frozen in liquid nitrogen or were embedded in GSV-1 tissue-embedding medium (SLEE Technik, Mainz, Germany), snap-frozen in liquid nitrogen-cooled isopentane, and stored at −70°C. Cryostat sections (10 μm) were mounted onto polylysine-coated slides and stored at −20°C. Paraffin-embedded brains from neonatally infected rats were prepared as described previously (69). Besides 4% buffered paraformaldehyde, Bouin's fixative (7 parts saturated picric acid, 5 parts 37% [wt/vol] formaldehyde, 1 part glacial acetic acid) was also used for perfusion of rats. For preparation of paraffin-embedded tissue from rats infected as adults, the animals were euthanized with CO_2 and immediately perfused transcardially with sterile phosphate-buffered saline (PBS) followed by 4% buffered paraformaldehyde. The brains were removed, fixed in 4% buffered paraformaldehyde for 24 h, dehydrated, and embedded in paraffin. Mice were sacrificed under ether anesthesia. One complete brain hemisphere was frozen in liquid nitrogen and stored at −70°C until RNA was prepared. The other brain hemisphere was fixed in Zamboni's reagent and embedded in paraffin (33). Approximately 8-μm-thick sagittal sections were mounted onto polylysine-coated slides and dried overnight at 37°C.

Preparation of RNA. Total RNA from cerebella, hippocampi, and frontal cortices of neonatally infected rats was prepared as described elsewhere (69). Total RNA from cerebra (excluding the cerebella) of rats infected as adults and from complete cerebra of infected mice was isolated using Trizol reagent (Life Technologies). Tissue homogenization was done with Trizol reagent (1 ml/100 mg of tissue) by vigorous vortexing and passages through 21- and 26-gauge needles. Precipitated RNA samples were dissolved in 0.5 mM EDTA and stored at −70°C.

Plasmid constructs. To generate the rat chemokine probes used for the RNase protection assay (RPA) and ISH, total RNA prepared from the brain of a Lewis rat infected with BDV at the age of 4 weeks and killed 33 days p.i. was reverse transcribed using oligo(dT). The resulting cDNA product was used for PCR amplification of fragments of the rat chemokines lymphotactin, MIP-1β, MCP-1, RANTES, and Mob-1/IP-10, the rat homologue of IP-10 (52, 60). Plasmid RPL32 (69) was used for PCR amplification of a fragment of the mouse housekeeping gene ribosomal protein L32. PCR amplification of a fragment of the gene coding for the delta chain of the mouse T-cell receptor–CD3 complex (T3δ gene) was done using cDNA obtained from total RNA prepared from the brain of a diseased BDV-infected MRL mouse. Specific primers flanked by *Hin*dIII (sense primer) and *Eco*RI (antisense primer) sites were used. PCR fragments were cloned into the pGEM-3Z vector (Promega), and their identities were verified by sequence analysis. All sequences were as published before (Table 1), except for two single nucleotide exchanges in the lymphotactin cDNA. Plasmids pMulL-1β and pMuTNFα, used for RPA to detect transcripts of mouse interleukin 1β (IL-1β) and tumor necrosis factor alpha (TNF-α), were kindly provided by Monte Hobbs (40). Sequences and lengths of the subcloned gene fragments, restriction enzymes, and polymerases used for generating antisense and sense RNA probes for RPA and ISH are listed in Table 1.

RPAs. To generate the rat chemokine multiprobe set, plasmids encoding the various chemokines and L32 were linearized using the restriction enzymes indicated in Table 1. L32 was included in the riboprobe set to detect transcripts of the ribosomal protein L32 (encoded by a housekeeping gene), permitting normalization of chemokine mRNA expression. Purified linearized DNAs were pooled at a concentration of 50 ng each per μl. The radiolabeled antisense RPA probe set was synthesized in a volume of 20 μl containing 100 μCi of [α-^{32}P]UTP (3,000 Ci/mmol); dithiothreitol (200 nmol); transcription buffer (Promega); 1 μl of template DNA; rUTP (61 pmol); rGTP, rATP, and rCTP (2.75 nmol each); RNase inhibitor (28 U; Pharmacia); and T7 polymerase (20 U; Promega). After 1 h of incubation at 37°C, the template DNAs were digested by treatment with DNase I (4 U; Ambion) for 30 min at 37°C. After extraction with phenol-chloroform, probes were precipitated with ethanol in the presence of mussel glycogen (20 μg; Roche Molecular Biochemicals), dried, and dissolved (3×10^5 cpm/μl) in hybridization buffer 1 [40 mM piperazine-*N*,*N*′-bis(2-ethanesulfonic acid) (PIPES) [pH 6.4], 0.4 M NaCl, 1 mM EDTA, 80% formamide]. Target RNA (10 μg) was dried under vacuum and resuspended in 15 μl of hybridization

buffer 1 containing 6×10^5 cpm of radiolabeled probe. Samples were denatured at 93°C for 3 to 4 min, slowly cooled to 56°C, and then incubated at 56°C in a hybridization oven for 14 to 18 h. Unprotected RNA was eliminated by the addition of 280 μl of a mixture containing RNase A (43 μg/ml; Sigma) and RNase T_1 (71 U/ml; Ambion) in 375 mM NaCl–5 mM EDTA (pH 8.0)–10 mM Tris-HCl (pH 7.5 to 8.0). After 60 min at 30°C, RNases were inactivated by the addition of 30 μl of a mixture containing sodium dodecyl sulfate (6.6%), proteinase K (1.7 mg/ml), and *Escherichia coli* tRNA (330 μg/ml; Roche Molecular Biochemicals) and incubation at 37°C for 30 min. After phenol-chloroform extraction, the protected RNA was precipitated with ethanol, dried, resuspended in loading buffer (80% formamide, 0.1% [wt/vol] xylene cyanol, 0.1% [wt/vol] bromphenol blue, 2 mM EDTA [pH 8.0]), and separated by 8 M urea–polyacrylamide gel electrophoresis. Dried gels were exposed first to phosphorimager plates and subsequently to Biomax films (Kodak).

RPAs using plasmids encoding BDV p40, rat Mob-1/IP-10, and rat T3δ sequences (see Fig. 2) as well as RPAs using plasmids encoding mouse T3δ, TNF-α, and IL-1β sequences (Table 1) were done as described previously (69). To measure chemokine gene expression in RNA prepared from infected mouse brains, a commercial mouse chemokine RPA multiprobe set (mCK-5 probe set; Pharmingen) was used. Synthesis of radiolabeled RNA transcripts and the subsequent RPA were carried out as suggested by the manufacturer.

IHC. Immunohistochemical analysis (IHC) was performed with mouse monoclonal antibody (MAb) W3/13 (anti-CD43; Harlan-Seralab, Leicestershire, England), specific for rat T lymphocytes (78). Cryostat sections were fixed for 10 min in ice-cold acetone and blocked in PBS–5% horse serum for 30 min, followed by incubations in avidin- and biotin-blocking solutions (10 min each; Vector Laboratories, Burlingame, Calif.). After three washes in PBS, sections were incubated with MAb W3/13 (diluted 1:600 in PBS–5% horse serum) overnight at 4°C. Sections were subsequently incubated for 30 min at room temperature with a biotinylated secondary horse anti-mouse antibody (rat adsorbed) (Vector Laboratories) diluted 1:200 in PBS–5% horse serum. Bound antibody was detected with an avidin-biotin-peroxidase kit (ABC; Vector Laboratories) and diaminobenzidine as a substrate. Sections were counterstained by immersion in Mayer's hematoxylin (Sigma), dehydrated in graded alcohols, and mounted in Entellan (E. Merck AG, Darmstadt, Germany). Thin sections of paraffin-embedded mouse brains were stained for BDV antigens as described previously (33).

ISH and combined ISH-IHC. ISH was performed as described by Simmons et al. (72) with minor modifications. Briefly, paraffinized sections were deparaffinized and rehydrated in graded alcohols. Sections then were postfixed in PBS–4% formaldehyde, treated with proteinase K (2.4 mg/100 ml of 5× Tris-EDTA buffer [1× Tris-EDTA is 10 mM Tris-Cl and 1 mM EDTA, pH 8.0]) for 15 min at 37°C, and acetylated (250 μl of acetic anhydride in 100 ml of PBS) for 10 min. After another 5-min fixation in PBS–4% formaldehyde, slides were dehydrated in graded alcohols and dried. For synthesis of the sense and antisense Mob-1/IP-10 and Crg-2/IP-10 (the mouse homologue of IP-10) probes, the reaction mixtures (6.26 μl) contained 125 μCi of [α-^{33}P]UTP (1,000 to 3,000 Ci/mmol); ATP, GTP, and CTP (1.55 nmol each); transcription buffer; RNase inhibitor (9 U); SP6, T7, or T3 RNA polymerase (7 U each; Promega); and 0.5 μg of template linearized with the appropriate restriction enzyme (Table 1). After incubation at 37°C for 90 min, DNA templates were digested for 30 min at 37°C by the addition of DNase I (0.7 U). Probes were ethanol precipitated, dried, and resuspended in 64 μl of 1× Tris-EDTA buffer containing 28 U of RNasin inhibitor (Pharmacia). Specific activities of the probes were calculated, and the slides were incubated at 56°C overnight in 100 μl of hybridization buffer 2 (50% formamide, 10 mM EDTA, 10% dextran sulfate, Denhardt's solution, 10 mM dithiothreitol, 2× SSPE [1× SSPE is 0.18 M NaCl, 10 mM NaH_2PO_4, and 1 mM EDTA {ph 7.7}], 100 μg of *E. coli* tRNA) containing 25 ng of probe (approximately 1.5×10^7 dpm). After digestion with RNase A (20 μg/ml), the slides were washed in decreasing concentrations of SSC (0.15 M NaCl plus 0.015 M sodium citrate). Slides were then either directly dehydrated in graded alcohols or further processed for IHC before dehydration.

Staining of sections with a mouse MAb to Calbindin-D (Sigma) at a 1:200 dilution was done as described for MAb W3/13. For staining with rabbit polyclonal sera against GFAP (glial fibrillary acid protein; DAKO, Hamburg, Germany) and BDV p40 (kindly provided by I. Lipkin, Irvine, Calif.), PBS–5% goat serum was used for blocking and for dilution of antibodies (1:500 [anti-BDV p40] or 1:1,000 [anti-GFAP]). The secondary antibody (biotinylated goat anti-rabbit; Vector Laboratories) was used at a 1:200 dilution. Dehydrated slides were air dried and exposed for 4 to 5 days to Ultra Vision G film (Sterling, Newark, Del.). The slides then were dipped in Kodak NTB-2 emulsion, dried, and stored in the dark for 4 weeks. Subsequently, the slides were developed, counterstained with Mayer's hematoxylin, mounted, and examined by dark- and bright-field microscopy.

Software and data processing. Autoradiographs and slides obtained from ISH studies were scanned, and composite images were generated using Photoshop (Adobe Systems, Mountain View, Calif.) and Microsoft Powerpoint software. For quantitative analysis of RPA results, dried gels were exposed to phosphorimager plates, and quantification was done using Macbas software (Fuji Photo Film Co., Tokyo, Japan). Graphic data were presented using Sigma Plot software (SPSS, Chicago, Ill.).

RESULTS

Chemokine gene expression in BDV-infected rat brains seems to immediately precede brain inflammation and onset of clinical symptoms. To study chemokine gene expression in the CNS of rats, we developed a suitable RPA multiprobe set which allows the simultaneous analyses of transcripts of the rat chemokine genes for lymphotactin, MIP-1β, RANTES, MCP-1, and Mob-1/IP-10 (here designated IP-10) (Table 1). To analyze cerebral chemokine gene expression at the earliest stages after intracerebral infection of adult rats, BDV-infected and mock-infected control rats were sacrificed at different times after infection, and total RNA prepared from the right brain hemispheres (excluding cerebella) was analyzed by RPA (Fig. 1). We found markedly increased transcription of all chemokine genes after day 10 p.i., predominantly for IP-10 and MCP-1 and to a lesser extent for MIP-1β, RANTES, and lymphotactin. While the amounts of IP-10, MCP-1, and MIP-1β transcripts measured at day 11 p.i. were already maximal, the amounts of RANTES and lymphotactin transcripts reached maximal levels only at about 3 weeks p.i. At all times, IP-10 gene expression was most prominent. Since lymphotactin is mainly produced by T cells and NK cells (36), its expression is likely to reflect the degree of CNS infiltration with lymphocytes. In brain samples from mock-infected animals, only very low levels of chemokine gene transcripts were detected at all times analyzed.

All animals were monitored at least twice daily for neurological symptoms. Until day 10 p.i., no clinical symptoms were observed. First signs of abnormal behavior, such as stereotypical head jerking, indicative of early BD, were generally noted after day 11 p.i.; the exception was one animal that did not exhibit detectable clinical symptoms until it was sacrificed at day 21 p.i.

Several chemokines can be produced by both leukocytes and CNS-resident cells (reviewed in references 5 and 38). To monitor the kinetics of leukocyte infiltration in infected brains, cryostat sections were analyzed with MAb W3/13, specific for CD43, which is expressed on the majority of mature T cells (78). Only a few meningeal CD43-positive cells were present in the sections at days 6 and 8 p.i., with no obvious differences compared to the results for control sections from mock-infected rats (data not shown). On days 9 and 10 p.i., in one of the two rats examined at each time, slight increases in the numbers of CD43-positive cells were observed in the meninges and in some cerebral vessels but not in the parenchyma. Consistent with previous reports (20), after day 11 p.i., large numbers of CD43-positive cells were present in perivascular infiltrates and, to a lesser extent, in the parenchyma of all animals (data not shown). Thus, the marked increase in chemokine gene expression after day 10 p.i. seemed to coincide with the initial appearance of perivascular infiltrates which, in turn, immediately preceded the onset of clinical symptoms.

To determine whether chemokine synthesis may actually precede inflammation, an RPA was performed to simultaneously detect IP-10 transcripts and, as a marker for T cells, T3δ transcripts. To account for possible differences between individual animals, we further increased the number of animals per time point. None of the additional BDV- and mock-infected rats sacrificed at day 6, 8, or 9 p.i. displayed any neurological symptoms. As shown in Fig. 2, one of three animals sacrificed at day 6 p.i., five of five animals sacrificed at day 8 p.i., two of five animals sacrificed at day 9 p.i., and two of two animals sacrificed at day 10 p.i. clearly contained higher levels of IP-10 transcripts in their brains than did age-matched control animals. Most of these animals also showed enhanced

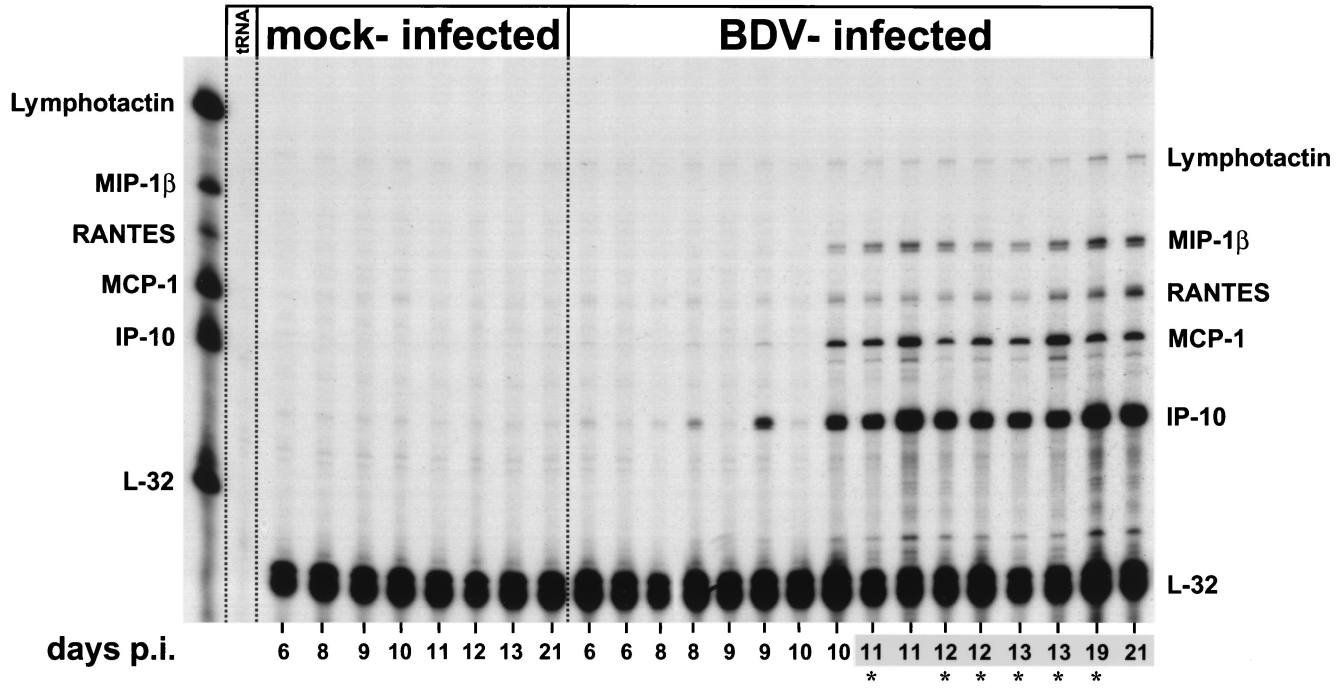

FIG. 1. Kinetics of expression of various chemokine genes in brains of adult BDV-infected rats. RNA samples (10 μg) from the right brain hemispheres (excluding cerebella) of mock- and BDV-infected rats sacrificed at different times p.i. were subjected to RPA using the rat chemokine probe set. *E. coli* tRNA (10 μg) was analyzed as a negative control. Positions of the various undigested probes are indicated on the left; positions of the protected probes are given on the right. The autoradiograph was exposed for 2 days. Numbers shaded in gray indicate brains which displayed perivascular infiltrates, as assessed by hematoxylin staining of frozen sections derived from the left brain hemispheres. Asterisks indicate rats which exhibited clinical symptoms of BD.

levels of T3δ transcripts, indicating that the inflammatory process had already started in these animals. Interestingly, however, a few animals synthesized IP-10 RNA in the absence of enhanced levels of T3δ transcripts, indicating that chemokine synthesis may precede inflammation. In parallel with the occurrence of inflammatory infiltrates after day 10 p.i., T3δ transcript levels strongly increased after this time and reached a maximum at day 21 p.i., the last time analyzed (Fig. 2 and data not shown).

To correlate chemokine gene expression with viral load, we performed an RPA to measure levels of transcripts encoding the BDV nucleoprotein p40. Viral transcripts were detected at all times after day 6. We noted considerable heterogeneity in levels of expression of viral markers between animals (Fig. 2), and BDV p40 RNA levels did not strictly correlate with IP-10 RNA levels.

Sustained chemokine gene expression in brains of neonatally infected rats in the absence of inflammation. The observed induction of IP-10 gene expression prior to the upregulation of T3δ mRNA in some adult-infected rats suggested that IP-10 was, at least in part, expressed by CNS-resident cells such as astrocytes. To examine chemokine gene expression in BDV-infected rat brains in the absence of encephalitis and gross inflammation, we took advantage of the persistent tolerant infection of the newborn rat (PTI-NB) model (13). In this model, virus persists in the CNS following perinatal infection, and the rats exhibit a split tolerance characterized by the virtual absence of a cellular immune response while the humoral response is still functional. As previously reported (42, 69), a mild transient infiltration of the CNS with mononuclear cells, mainly restricted to the cortex, was observed between 22 and 33 days after neonatal infection. Inflammatory infiltrates were absent at later times, and parenchymal immune cells were found only sporadically.

For analysis of chemokine gene expression, we used archival RNA samples derived from the frontal cortices, cerebella, and hippocampi of neonatally infected and mock-infected rats that were sacrificed at different times p.i., ranging from 8 to 135 days. These RNA samples were shown to contain only minute amounts of T3δ RNA (reference 69 and data not shown). Analysis of these RNA samples by RPA revealed that brains of PTI-NB rats exhibited elevated levels of chemokine transcripts, predominantly IP-10 and RANTES, in the cortex and cerebellum (quantitative analyses shown in Fig. 3A and B, respectively) and in the hippocampus (only data at 2.5 and 4.5 months p.i. were available; data not shown). The high level of expression of IP-10 in the frontal cortex at day 22 p.i. was likely due to the above-mentioned transient inflammation. IP-10 gene expression levels in PTI-NB rats declined at later times but remained at least 25% the value measured in whole-brain

FIG. 2. Semiquantitative analysis of IP-10, T3δ, and BDV p40 gene expression in brains of mock- and BDV-infected rats. RNA samples (10 μg) from the right brain hemispheres (excluding cerebella) of mock- and BDV-infected rats sacrificed at different times p.i. were subjected to RPA using probes for IP-10 (upper panel), T3δ (middle panel), and BDV p40 (lower panel). The two upper autoradiographs were derived from the same RPA gel; they were exposed for 12 days. The lower autoradiograph was exposed for 5 days. For quantification, the dried RPA gels were exposed to phophorimager plates, and the band intensities were determined using Macbas software. Bars indicate relative RNA contents (arbitrary units) calculated by normalizing the band intensities against the corresponding L32 transcript levels (data not shown). A logarithmic scale was chosen for the presentation of IP-10 and T3δ RNA levels, with cutoff values of 0.35 for IP-10 and 0.13 for T3δ.

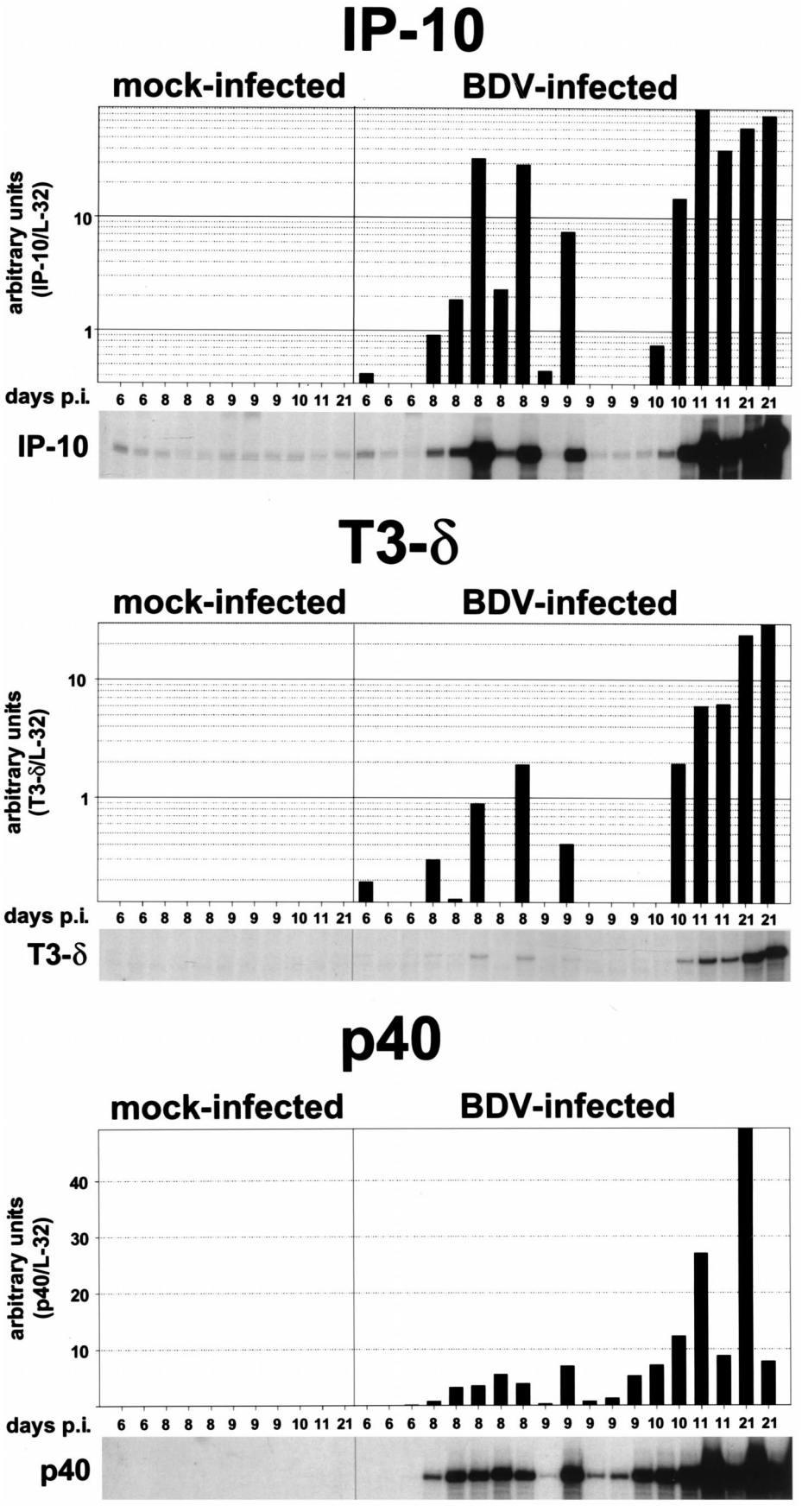
IP-10
mock-infected
BDV-infected
arbitrary units (IP-10/L-32)
10
1
days p.i.
6 6 8 8 8 9 9 9 10 11 21 6 6 6 8 8 8 8 9 9 9 9 9 10 10 11 11 21 21
IP-10
T3-δ
mock-infected
BDV-infected
arbitrary units (T3-δ/L-32)
10
1
days p.i.
6 6 8 8 8 9 9 9 10 11 21 6 6 6 8 8 8 8 9 9 9 9 9 10 10 11 11 21 21
T3-δ
p40
mock-infected
BDV-infected
arbitrary units (p40/L-32)
40
30
20
10
days p.i.
6 6 8 8 8 9 9 9 10 11 21 6 6 6 8 8 8 8 9 9 9 9 9 10 10 11 11 21 21
p40

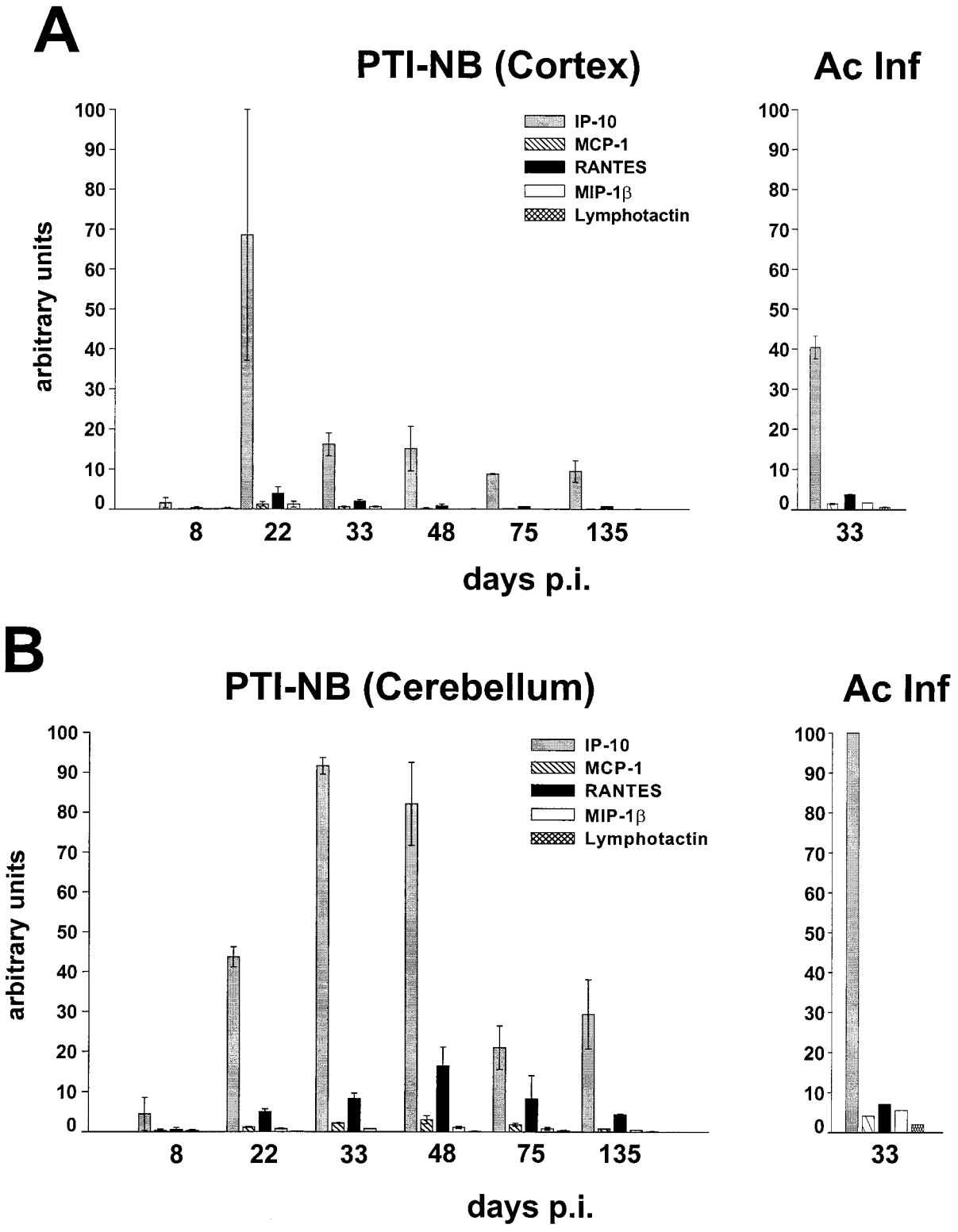

FIG. 3. Semiquantitative analysis of chemokine gene expression in different rat brain regions following perinatal BDV infection. (A) RNA samples (10 μg) from the frontal cortices of neonatally mock- or BDV-infected (PTI-NB) rats sacrificed at different times p.i. (two animals per time point) were subjected to RPA using the rat chemokine probe set. Samples of brain RNA (10 μg) isolated at 33 days p.i. from two adult rats (acute BDV infection [Ac Inf]) served as positive controls. The dried gel was exposed to a phosphorimager plate, and band intensities were quantified using Macbas software. Bars represent means and standard errors of the means after normalization against L32 transcript levels (arbitrary units). (B) Semiquantitative analysis of chemokine gene expression in the cerebella of PTI-NB rats at different times p.i., as assessed by RPA. Experimental procedures and quantification were as described for panel A. We also analyzed brain tissue from one rat infected as an adult and sacrificed 33 days p.i. (Ac Inf). In both the frontal cortex and the cerebellum, chemokine values for mock-infected rats were lower than the respective day-8 values for PTI-NB rats (data not shown).

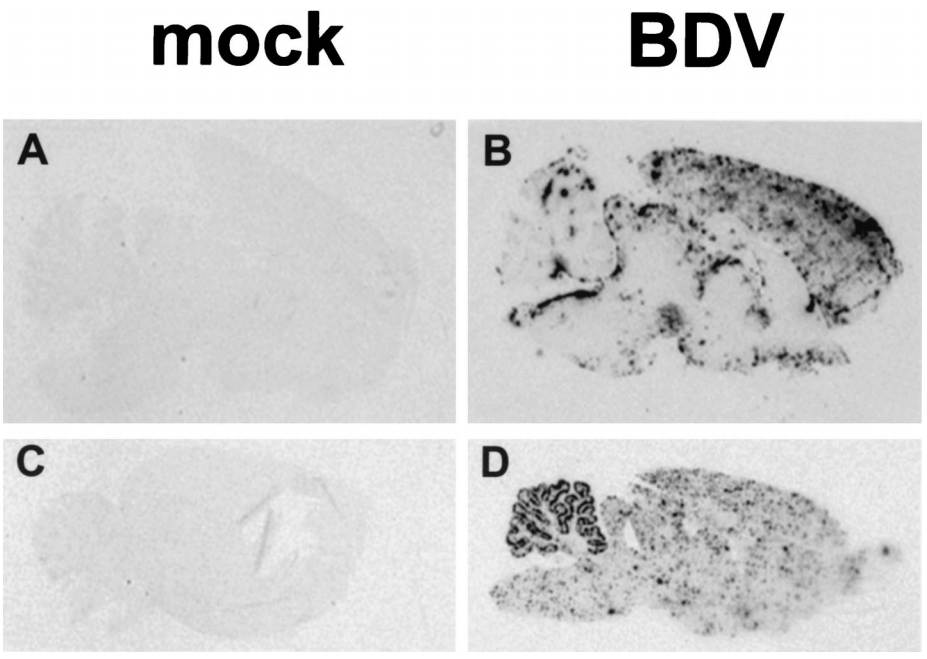

FIG. 4. Localization of IP-10 expression in BDV-infected rat brains. Rats were both mock infected and infected with BDV as adults (A and B) or neonates (C and D) and sacrificed 12 days (A and B) or 75 days (C and D) later. Following perfusion of rats with fixative, their brains were removed, dehydrated, and embedded in paraffin. Sagittal sections derived from these brains were probed with a ^{33}P-labeled antisense riboprobe specific for rat IP-10 transcripts. Shown are scanned autoradiographs after 5 days of exposure to film. Note the characteristic distribution of signals in the cerebellum of the neonatally infected rat (D) as well as the strong signals localized in the neocortex of the rat infected as an adult (B). The specificity of the ISH signals is demonstrated by the absence of specific signals in sections from mock-infected rats (A and C).

extracts from infected adult animals sacrificed at day 33 p.i. (Fig. 3). Inflammatory infiltrates were virtually absent after day 33 p.i., and T3δ gene expression levels were only marginally increased compared to those in mock-infected control animals (69). These findings strongly suggested that CNS-resident cells represent the major source of chemokine transcripts at these later times.

Identification of IP-10 gene-expressing cells in BDV-infected rat brains by ISH. To determine the cell type expressing IP-10 in BDV-infected rat brains, we performed combined ISH and IHC examinations. We decided to concentrate on the IP-10 gene, since RPA data revealed that this gene is expressed most strongly and at the earliest times in BDV-infected rat brains. ISH studies done on CNS sections derived from adult rats sacrificed 11 or 12 days p.i. showed strong hybridization signals in the cortex and the meninges (Fig. 4B), whereas there were no signals in brains of mock-infected animals (Fig. 4A). Hybridization of sections using the IP-10 sense probe did not yield specific signals, demonstrating the specificity of the IP-10 antisense probe (data not shown). IHC staining of sections with a serum against BDV p40 combined with ISH revealed a good overall association between antigen-positive and ISH-positive regions (data not shown). Combined ISH for IP-10 and IHC for GFAP revealed that astrocytes represented the predominant cell type that expressed IP-10 in inflamed brains of adult rats (Fig. 5A). Strong IP-10 signals were also detected in perivascular infiltrates. They may have originated from endothelial cells or blood-derived immune cells, such as activated T cells, NK cells, and macrophages. The identity of additional parenchymal GFAP-negative cells that expressed IP-10 remains unclear (Fig. 5A and data not shown).

ISH performed on sections of paraffin-embedded PTI-NB rat brain tissues representing different days p.i. (14, 22, 33, 48, 75, and 135) showed that hybridization signals were strongest in these animals at day 22 p.i. and declined somewhat at later times (Fig. 4D and data not shown). In the forebrain, IP-10-expressing cells were predominantly found in clusters that were fairly homogeneously dispersed (Fig. 4D and 5B). In contrast, in the cerebellum of PTI-NB rats, hybridization signals appeared to be mainly restricted to the gray matter, where signals were also most intense (Fig. 4D and 5C and D). Microscopic analysis of ISH slides showed a characteristic localization of IP-10 signals in the cerebellum: IP-10-positive cells were predominantly observed in the Purkinje cell layer (Fig. 4C and D), suggesting that Purkinje cells represent the source of IP-10 mRNA. However, combined ISH for IP-10 and IHC for Calbindin-D, a specific marker for Purkinje cells (51), indicated that GFAP-immunoreactive Bergmann glia, localized in immediate proximity to Purkinje cells, was the site of strong IP-10 gene expression (Fig. 5C, E, and F). This characteristic pattern of IP-10 gene expression confined to the Purkinje cell layer was noted at all times after day 22 p.i. (data not shown).

Chemokine synthesis in brains of BDV-infected mice. Using a commercially available RPA kit which permits the simultaneous detection of transcripts from nine different chemokine genes, we determined their expression patterns in brains of infected MRL mice, which are highly susceptible to BDV-induced neurological disease (33). We found that the RANTES and Crg-2/IP-10 genes were already expressed at 20 and 24 days p.i., when the animals did not yet exhibit clinical symptoms (data not shown). In brains of diseased mice sacrificed at later times, we also found transcripts for lymphotactin, MIP-1β, MIP-1α, MCP-1, and MIP-2. These results indicated that the rat and mouse models yielded comparable results regarding chemokine gene expression in brains after infection with BDV.

We next studied the kinetics of chemokine gene expression in brains of BDV-infected mice that cannot mount an effective

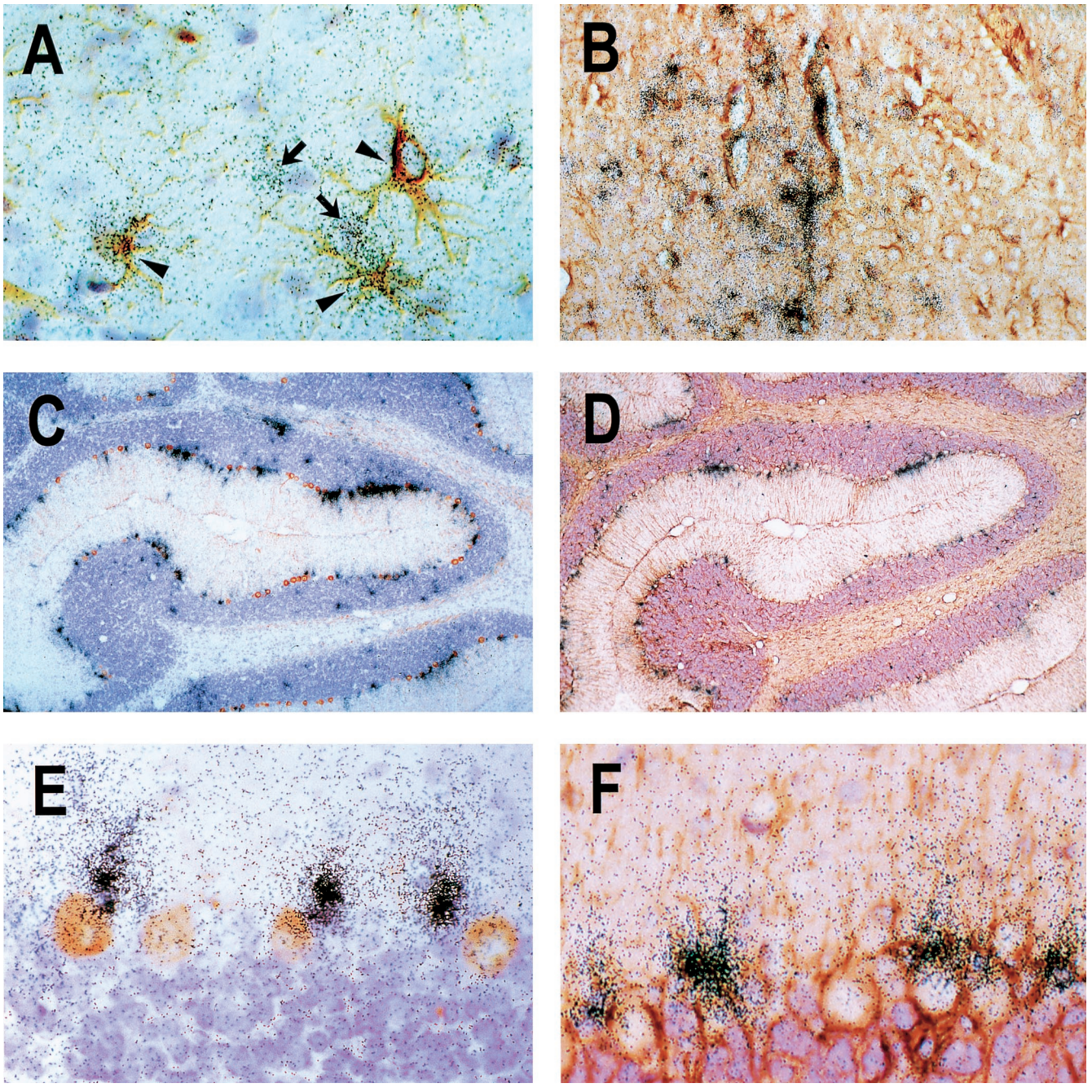

FIG. 5. Astrocytic IP-10 gene expression in the CNS of BDV-infected rats. Rats were infected as adults (A) or neonates (B to F) and euthanatized 11 days (A), 33 days (C to F), or 75 days (B) later. Following perfusion of rats using either 4% buffered paraformaldehyde (A) or Bouin's fixative (B to F), brains were removed and processed for analysis by ISH. ISH with a ^{33}P-radiolabeled IP-10 antisense probe was combined with IHC for GFAP as a marker for astrocytes (A, B, D, and F) or Calbindin-D as a marker for Purkinje cells (C and E). Panels A and B depict representative cortical regions. Arrowheads indicate ISH-positive astrocytes, whereas arrows indicate GFAP-negative cells of unknown identity that express IP-10. In panels C and D, parts of the cerebellum from two consecutive sections are shown. Note the string-like distribution of IP-10 signals in the Purkinje cell layer. High-power magnifications of the Purkinje cell layer are shown in panels E and F. Original magnifications were ×20 (C and D), ×80 (B and F), and ×200 (A and E).

antiviral immune response. Mutant mice lacking β2-microglobulin ($\beta2m^{0/0}$ mice) fail to express major histocompatibility complex class I complexes and therefore lack $CD8^+$ T cells, which are the main effector cells in the BDV-induced neuropathological process (33, 35). When brains of persistently infected, clinically healthy $\beta2m^{0/0}$ MRL mice were analyzed for chemokine gene expression, it was evident that Crg-2/IP-10 and RANTES transcripts were abundantly present at all times from 4 to 13 weeks p.i. (Fig. 6). Brains of these mice also contained slightly elevated levels of MCP-1, MIP-1α, and MIP-1β transcripts. Enhanced levels of MIP-2 and lymphotactin transcripts were found only in animals that were infected for 9 or more weeks. Lymphotactin was presumably synthesized by $CD4^+$ T cells, which can be found rather frequently at

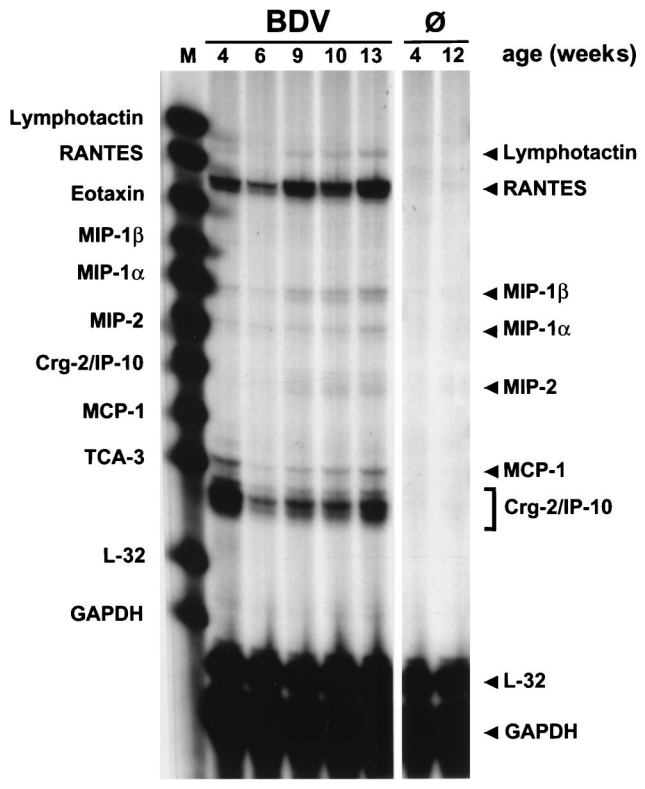

FIG. 6. Sustained expression of chemokine genes in brains of disease-resistant $\beta 2m^{0/0}$ MRL mice. Animals infected as newborns were analyzed at the indicated ages. RNA samples (10 μg) prepared from one brain hemisphere each were subjected to RPA using the mCK-5 probe set, designed to simultaneously detect transcripts of nine chemokine genes and the L32 and glyceraldehyde-3-phosphate dehydrogenase (GAPDH) housekeeping genes. Brain RNA from uninfected mice (Ø) served as a negative control for the various experiments. RPA products were separated on a 5% denaturing polyacrylamide gel and exposed to X-ray film. Positions of the undigested RNA probes, which served as size markers (M), are indicated on the left; arrowheads on the right indicate positions of the protected probes. Note that the Crg-2/IP-10 signals exhibited a smaller size than expected. This unusual signal pattern of Crg-2/IP-10 transcripts can be explained by a polymorphism in the Crg-2/IP-10 gene which results in RNase-resistant fragments of reduced size when material from MRL mice is analyzed with the mCK-5 probe set (32).

perivascular sites of mutant mice at late times of infection (unpublished observation). The presence of T cells was confirmed by RPA using a probe that specifically detects T3δ transcripts (data not shown).

To determine which cell type in the BDV-infected mouse brains was responsible for chemokine synthesis, we performed combined ISH and IHC experiments on paraffin-embedded sections of brains from infected $\beta 2m^{0/0}$ MRL mice with a riboprobe specific for Crg-2/IP-10 transcripts (Fig. 7). Typically, Crg-2/IP-10-positive cells were found in clusters of five or more cells (Fig. 7A). Such clusters of ISH signals were found in all regions of BDV-infected $\beta 2m^{0/0}$ MRL mouse brains. No specific ISH signals were found in brains of uninfected control mice. ISH signals were also absent in sections of infected brains treated with the radiolabeled Crg-2/IP-10 sense probe (data not shown). Careful histological examination of brain sections that were simultaneously stained for Crg-2/IP-10 transcripts by ISH and for BDV p40 by IHC revealed that high concentrations of silver grains were usually located over cells that showed no or very little viral antigen (Fig. 7B). Most Crg-2/IP-10-positive cells were GFAP-immunoreactive astrocytes (Fig. 7C), suggesting that these cells were the major source of Crg-2/IP-10 in brains of BDV-infected $\beta 2m^{0/0}$ MRL mice.

Chemokine synthesis in brains of infected triple knockout mice lacking mature B and T cells and functional IFN receptors. Crg-2/IP-10 gene expression in brains of BDV-infected $\beta 2m^{0/0}$ MRL mice might be triggered by cytokines released from lymphocytes in the CNS. To evaluate this possibility, we used triple knockout mice that lack mature B and T cells due to a targeted disruption of the Rag-2 gene and that have additional genetic defects that make them unresponsive to IFN-γ and IFN-α/β (AGR mice) (44). The latter defects resulted from targeted disruptions of genes encoding a subunit of the IFN-α/β receptor and a subunit of the IFN-γ receptor (58). Since newborn AGR mice were not available for these experiments, 4- to 6-week-old animals were infected intracerebrally with a variant of BDV strain He/80 that had been selected for rapid growth in adult mouse brains (P. Staeheli, unpublished results), and the mice were sacrificed 4 weeks later. We found that seven of the eight infected triple knockout mice contained elevated levels of Crg-2/IP-10 and RANTES in their brains, whereas chemokine gene transcripts were barely detectable in the last infected AGR mouse and in the two uninfected control mice (Fig. 8). Successful BDV infection of the eight mice was confirmed by both IHC and RPA (Fig. 9A and data not shown). Quantification showed that, on average, the infected AGR mice contained about eightfold-higher Crg-2/IP-10 RNA levels and about threefold-higher RANTES RNA levels than their uninfected littermates (Fig. 8), indicating that these two chemokine genes can be activated by BDV through unknown signaling pathways which do not involve IFNs or other factors secreted by T and B cells.

Crg-2/IP-10 is expressed by scattered astrocytes in brains of infected AGR triple knockout mice. To determine the cell type expressing IP-10 in brains of infected AGR triple knockout mice, we performed combined ISH and IHC examinations (Fig. 9). In contrast to the situation for the brains of infected $\beta 2m^{0/0}$ MRL mice, where Crg-2/IP-10-expressing astrocytes were frequently found in clusters, only scattered individual cells containing high levels of Crg-2/IP-10 RNAs were observed. They were present mainly in the hippocampus (Fig. 9), the brain area of maximal virus load, and less frequently in the neocortex (data not shown). Crg-2/IP-10-positive cells were mostly GFAP-immunoreactive astrocytes that were surrounded by astrocytes that did not express this chemokine (Fig. 9B). This pattern would be expected if viral components were able to activate unknown intracellular factors that promote transcription of the Crg-2/IP-10 gene.

Levels of expression of TNF-α and IL-1β are not enhanced in brains of infected AGR triple knockout mice. Besides IFN-α/β, and IFN-γ, proinflammatory cytokines, such as TNF-α and IL-1β, also have been shown to be capable of inducing astrocytic IP-10 gene expression, although with a lower efficiency (43). Triple knockout mice still possess functional NK cells, which are a possible source of proinflammatory cytokines (15). Since it was not known whether NK cells were present in the brains of infected AGR mice, we used RPA to analyze TNF-α and IL-1β expression levels in brains of infected AGR mice and control AGR mice. RNA from the brain of a BDV-infected MRL mouse with neurological disease was included in the assay as a positive control. While IL-1β was strongly expressed in the brain of the infected MRL mouse, IL-1β transcripts were detected neither in the infected AGR mice nor in the uninfected control AGR mice (data not shown). Consistent with previous reports (11), low levels of TNF-α transcripts were present in the brains of uninfected control mice. TNF-α expression levels in infected AGR mice were almost identical

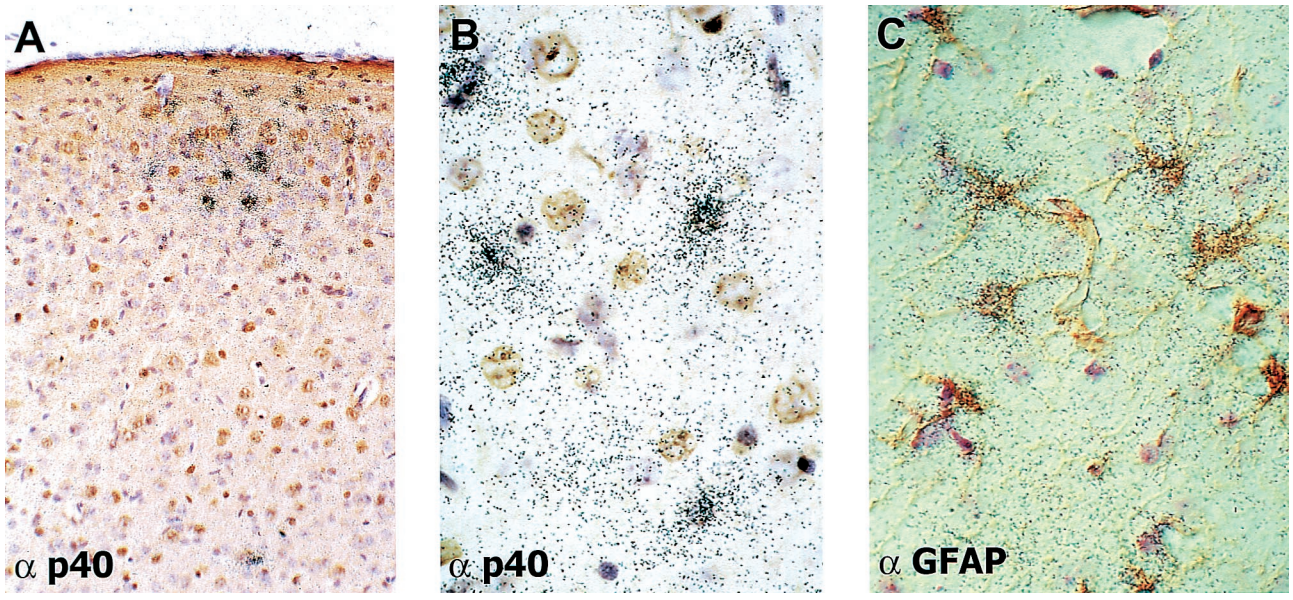

FIG. 7. Localization of Crg-2/IP-10 gene transcripts by ISH in brains of BDV-infected $\beta 2m^{0/0}$ MRL mice. Mice infected as newborns were sacrificed at 9 weeks of age, and one brain hemisphere each was fixed in Zamboni's fixative and processed for analysis by ISH with a ^{33}P-radiolabeled riboprobe specific for Crg-2/IP-10 transcripts. Brain sections were stained simultaneously with antisera (α) to BDV p40 (A and B) and GFAP (C). (A) Typical cluster of Crg-2/IP-10-positive cells in the neocortex at a low magnification. (B and C) Most Crg-2/IP-10-positive cells did not express detectable amounts of viral antigen (B), and high densities of silver grains were found most frequently over GFAP-positive cells (C). Magnifications, ~×54 (A) and ×134 (B and C) (original magnifications were ×80 [A] and ×200 [B and C]).

to those measured in the control mice. The mean value for TNF-α was 2.7 (standard deviation, 0.839) arbitrary units after normalization against L32 expression levels in the eight infected AGR mice; that in the two AGR control mice was 2.32 (standard deviation, 1.22) arbitrary units. In contrast, the TNF-α expression level in the diseased MRL mouse was about 25-fold higher than that in the control mice. Thus, TNF-α and IL-1β did not seem to contribute significantly to chemokine gene expression in the brains of infected AGR mice.

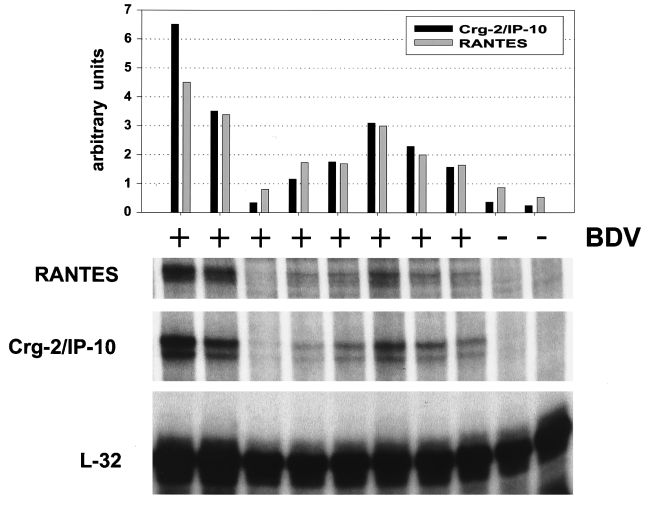

FIG. 8. Expression of the Crg-2/IP-10 and RANTES genes in brains of BDV-infected triple knockout mice lacking mature B and T cells and functional IFN-α/β and IFN-γ receptors. Mice were either infected with BDV (+) at 4 to 6 weeks of age or were left uninfected (−). They were sacrificed 4 weeks later. To detect chemokine transcripts, RPA was done as described in the legend to Fig. 6. To visualize Crg-2/IP-10 and RANTES transcripts, the autoradiograph was exposed for 9 days. Exposure time for the autoradiograph with L32 transcripts was 16 h. Crg-2/IP-10 and RANTES signals were quantified using a phosphorimager. Bars depict Crg-2/IP-10 and RANTES transcript levels normalized against L32 RNA levels (arbitrary units).

DISCUSSION

A complex pattern of chemokine gene expression was previously observed for CNS inflammatory diseases induced by either human immunodeficiency virus (HIV) or simian immunodeficiency virus (67, 68, 70), mouse hepatitis virus (MHV) (50), lymphocytic choriomeningitis virus (LCMV) (1, 3), Theiler's murine encephalomyelitis virus (TMEV) (41), and mouse adenovirus type 1 (16). Only very limited information has been available to date regarding the role of chemokines in BDV-induced CNS disease. MIP-1β and IP-10 transcripts were previously found in brains of BDV-infected adult rats, irrespective of treatment with the immunosuppressive agent dexamethasone (57). Here, we used RPA technology to simultaneously measure transcript levels of several chemokine genes in brains of rats and mice infected with BDV under conditions that resulted either in fulminant neurological disease or in tolerance of persistent infection without disease.

An important finding of this study was that increased IP-10 gene expression in the brains of some rats infected as adults was already observed at about day 8 p.i., when no signs of inflammation were detected by immunohistological and molecular biological methods. Additionally, in brains from PTI-NB rats, we measured prominent sustained expression of the IP-10 gene despite the virtual absence of immune cell infiltrates. Similarly, transcripts of RANTES and Crg-2/IP-10 were present in brains of mutant mice lacking functional $CD8^+$ T cells. These data suggested that brain-resident cells represent the major source of chemokines in our model system. This view was supported by ISH studies which showed that astrocytes synthesized IP-10 transcripts in both the presence and the absence of inflammatory infiltrates in rat and mouse brains. Our findings thus support the proposed role of chemokines in lymphocyte and macrophage recruitment to the brain follow-

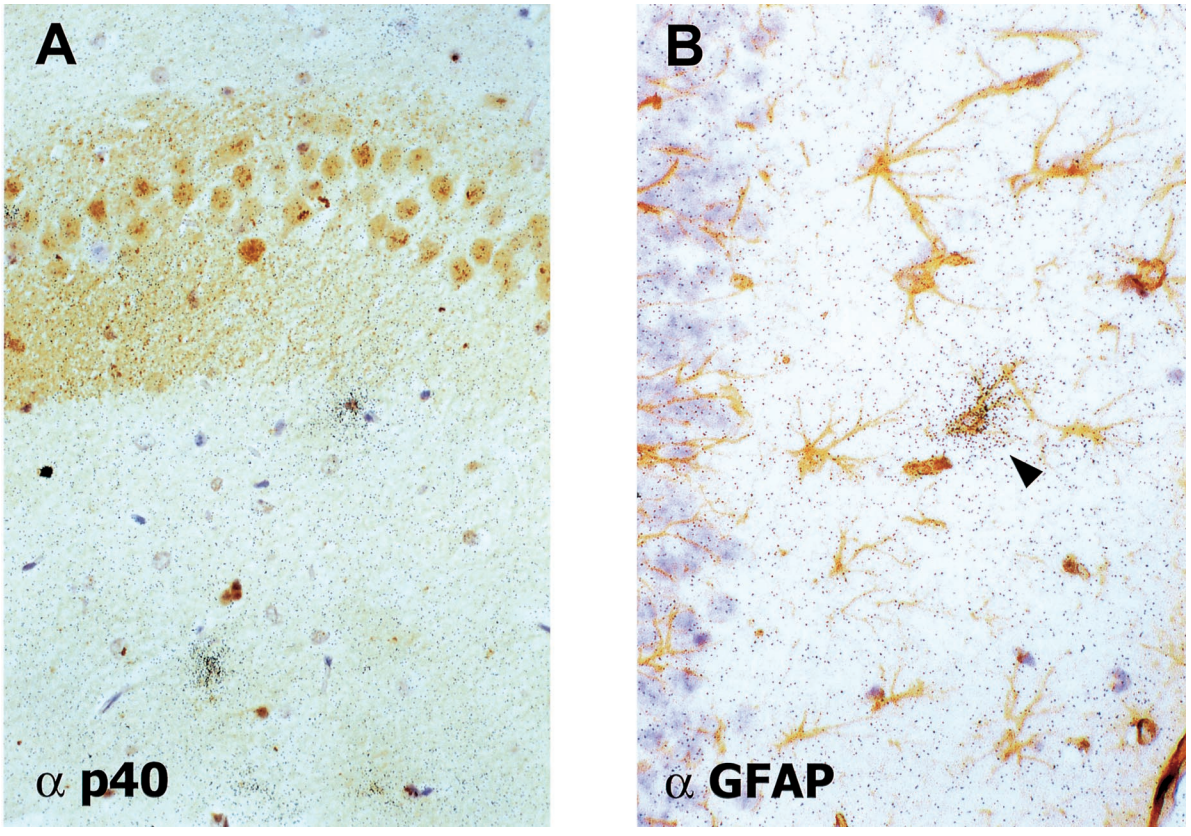

FIG. 9. Scattered distribution of astrocytes expressing the Crg-2/IP-10 gene in brains of BDV-infected triple knockout mice. A paraffin-embedded brain hemisphere of an infected mouse sacrificed 4 weeks p.i. was subjected to ISH with a ^{33}P-radiolabeled riboprobe specific for Crg-2/IP-10 transcripts and immunostaining with antiserum (α) to either BDV p40 (A) or GFAP (B). Some scattered Crg-2/IP-10-positive cells were present in the hippocampus (A and B). High concentrations of silver grains were typically found over GFAP-positive cells (arrowhead in panel B). Magnification, ~×107 (original magnification, ×120).

ing virus infection of the CNS (3). Increased chemokine gene expression prior to significant CNS leukocyte infiltration and neurological disease has also been observed for mice infected with LCMV, MHV, and TMEV (1, 41, 50).

Lymphocyte recruitment was impaired in our PTI-NB rats despite sustained expression of the IP-10 gene and other chemokine genes, presumably because the T cells of these animals are tolerant to BDV antigens. It was previously shown that injection of IP-10 into the hippocampus of the mouse provoked no detectable leukocyte recruitment to the brain parenchyma (9), suggesting that this chemokine can induce only activated and not naive T cells to cross the blood-brain barrier. Consistent with this hypothesis, it has been shown that IP-10 is a strong chemoattractant for activated but not resting T cells (25).

Using the mouse model system, we tried to identify the factors required for the stimulation of chemokine gene expression in astrocytes of BDV-infected brains. IFN-γ, which can be secreted by T cells and NK cells, is a potent stimulator of IP-10 and RANTES gene expression in a variety of cells, including activated monocytes, T cells, endothelial cells, microglia, and astrocytes (26, 43, 55, 60, 76). Similarly, IFN-α/β has been shown to upregulate IP-10 and RANTES gene expression in human fetal microglia and astrocyte cultures (43) as well as in mouse fibroblasts (M. S. de Veer, S. Der, A. Zhou, R. H. Silverman, and B. R. G. Williams, personal communication) and macrophages (24).

Our work with triple knockout mice showed that B and T cells are not important for the initial stimulation of chemokine synthesis in BDV-infected brains. The results further demonstrated that IFN-γ, which might be secreted by NK cells, also does not play a critical role in this induction process. Consistent with this finding, it was found in the LCMV model system that infection of mice devoid of a functional IFN-γ gene resulted in decreased but not completely abrogated expression of IP-10, suggesting that additional factors are important for chemokine gene induction in LCMV-infected mouse brains (1). Finally, the results showed that IFN-α/β is not strictly required for Crg-2/IP-10 and RANTES expression in BDV-infected mouse brains.

ISH of brain sections from triple knockout mice revealed the presence of a few scattered astrocytes which strongly expressed Crg-2/IP-10. In contrast, fairly large clusters of Crg-2/IP-10-positive cells were typically present in mice with functional IFN-α/β receptors. These data suggested that virus-induced IFN might nevertheless serve to amplify Crg-2/IP-10 synthesis in BDV-infected brains.

The clustered occurrence of chemokine-producing astrocytes in BDV-infected brains of rats and mice indicated that infected neurons might not contribute significantly to the production of chemokine-inducing factors, because infected neurons were extremely abundant and distributed fairly evenly throughout the brains of our BDV-infected animals. If these factors were produced by these cells, chemokine synthesis should have been activated uniformly in all astrocytes. Since this was clearly not the case, it seems likely that the production of chemokine-inducing factors is limited to a rare subpopulation of virus-infected astrocytes and possibly other brain cells.

Since astrocytes were reported to express viral antigen at early times after infection of rats (14), it is reasonable to assume that BDV-infected astrocytes play a key role in early chemokine gene expression.

Apart from IFN-α/β, other cytokines, such as IL-1β and TNF-α, can induce the synthesis of IP-10 and RANTES in astrocytes (31, 38, 43, 61, 62). Since we and others previously demonstrated sustained expression of several proinflammatory cytokines in the brains of PTI-NB rats (42, 63, 69), it is likely that these molecules contributed to astrocytic chemokine gene expression in BDV-infected rats. Since our attempts to demonstrate increased expression of IL-1β and TNF-α transcripts in brains of BDV-infected AGR mice were not successful, it seems that, contrary to the situation in rats, these proinflammatory cytokines do not contribute significantly to chemokine synthesis in BDV-infected mouse brains.

Our observation that Crg-2/IP-10 was strongly expressed in some scattered astrocytes of AGR triple knockout mice implies that BDV can stimulate the expression of chemokine genes via a more direct, cytokine-independent mechanism which still remains to be defined. Other RNA viruses, such as MHV, Newcastle disease virus, and measles virus, were shown to induce IP-10 gene expression in primary rodent astrocytes (26, 50) and glioblastoma cells (59). Consistent with these findings, Hua and Lee (43) recently showed that synthetic double-stranded RNA was capable of inducing IP-10 gene expression in human fetal astrocyte cultures. Furthermore, HIV Tat was reported to induce IL-8 and IP-10 in primary human astrocytes (48). A recent report provided evidence that activation of the MCP-1 gene promoter results from the action of the HIV Tat protein in a human astrocytoma cell line (53). Moreover, Sendai virus-induced expression of RANTES in human embryonic kidney cells was shown to result from the activation of transcription factor IRF-3, which then recognizes a binding motif in the RANTES gene promoter (54).

An unexplained finding of our study was that the IP-10 gene was expressed more prominently than other chemokine genes in BDV-infected mouse and rat brains. A similar situation was found for brains of mice infected with LCMV, MHV, or mouse adenovirus type 1 (1, 16, 50). Moreover, the concentrations of IP-10 and MCP-1, but not other chemokines, were increased in the majority of cerebrospinal fluid samples from patients suffering from paramyxovirus- or enterovirus-induced meningitis (49). Likewise, IP-10 and MCP-1 were the only chemokines consistently detected in cerebrospinal fluid samples from HIV-infected patients (45). A common scheme thus emerges from these studies which points to an important role for IP-10 in virus-induced CNS inflammation. In this context, it is noteworthy that the overexpression of IFN-α/β in astrocytes of transgenic mice induced high levels of Crg-2/IP-10 transcripts and much lower levels of RANTES and MCP-1 transcripts (4).

In addition to the traditional role of leukocyte attraction, recent studies implicated chemokines in brain development and normal function, such as neuronal migration and neuronal signaling (reviewed in references 2 and 38). PTI-NB rats exhibit distinct behavioral disturbances and neuroanatomical abnormalities, including cerebellar hypoplasia (see references 12 and 29 for reviews). While it remains to be determined if the sustained upregulation of chemokines contributes to the behavioral and anatomical abnormalities observed in PTI-NB rats, our data suggest the possibility that enhanced expression of chemokines might contribute to the selective loss of cerebellar Purkinje cells in brains of PTI-NB rats (23, 42, 80). Purkinje cells are the first cells in the cerebellum to express viral antigen after perinatal infection of rats with BDV, and they remain the major cell type expressing viral antigen throughout the infection (7, 23). At about 3 to 4 weeks after infection, the Bergmann glia also is infected (7, 30). Our ISH experiments with brains from PTI-NB rats revealed extremely high levels of IP-10 transcripts in the Bergmann glia already at early times after infection. Thus, IP-10 induction might be a direct consequence of BDV infection of these cells or, alternatively, might be triggered by factors secreted from infected Purkinje cells. It is tempting to speculate that IP-10 represents an astrocytic alarm signal by which immune cells are recruited for the elimination of infected CNS cells. It is unclear whether blood-derived cells are involved in Purkinje cell death in our model system or whether the observed loss of neurons is due to toxic factors secreted by activated microglia and astrocytes (22, 27, 46).

ACKNOWLEDGMENTS

We thank Juan Carlos de la Torre for permission to use material generated in his laboratory; Martin Schwemmle, Juan Carlos de la Torre, and Otto Haller for critically reading the manuscript; Birgit Scherer for technical assistance; and Iain Campbell for providing the mouse Crg-2/IP-10 ISH probe.

This work was supported by grants from the Deutsche Forschungsgemeinschaft and the Zentrum für Klinische Forschung I of the Universitätsklinikum Freiburg. C.S. is a fellow of the German Stipendienprogramm Infektionsforschung, DKFZ, Heidelberg, Germany. L.B. was supported by a stipend from the Universitätsklinikum Freiburg.

REFERENCES

1. **Asensio, V. C., and I. L. Campbell.** 1997. Chemokine gene expression in the brains of mice with lymphocytic choriomeningitis. J. Virol. **71:**7832–7840.
2. **Asensio, V. C., and I. L. Campbell.** 1999. Chemokines in the CNS: plurifunctional mediators in diverse states. Trends Neurosci. **22:**504–512.
3. **Asensio, V. C., C. Kincaid, and I. L. Campbell.** 1999. Chemokines and the inflammatory response to viral infection in the central nervous system with a focus on lymphocytic choriomeningitis virus. J. Neurovirol. **5:**65–75.
4. **Asensio, V. C., S. Lassmann, A. Pagenstecher, S. C. Steffensen, S. J. Henriksen, and I. L. Campbell.** 1999. C10 is a novel chemokine expressed in experimental inflammatory demyelinating disorders that promotes recruitment of macrophages to the central nervous system. Am. J. Pathol. **154:** 1181–1191.
5. **Bacon, K. B., D. R. Greaves, D. J. Dairaghi, and T. J. Schall.** 1998. The expanding universe of C, CXC and CC chemokines, p. 753–775. *In* A. Thomson (ed.), The cytokine handbook. Academic Press, Inc., San Diego, Calif.
6. **Baggiolini, M., B. Dewald, and B. Moser.** 1997. Human chemokines: an update. Annu. Rev. Immunol. **15:**675–705.
7. **Bautista, J. R., S. A. Rubin, T. H. Moran, G. J. Schwartz, and K. M. Carbone.** 1995. Developmental injury to the cerebellum following perinatal Borna disease virus infection. Dev. Brain Res. **90:**45–53.
8. **Bazan, J. F., K. B. Bacon, G. Hardiman, W. Wang, K. Soo, D. Rossi, D. R. Greaves, A. Zlotnik, and T. J. Schall.** 1997. A new class of membrane-bound chemokine with a CX3C motif. Nature **385:**640–644.
9. **Bell, M. D., D. D. Taub, and V. H. Perry.** 1996. Overriding the brain's intrinsic resistance to leukocyte recruitment with intraparenchymal injections of recombinant chemokines. Neuroscience **74:**283–292.
10. **Bilzer, T., and L. Stitz.** 1996. Immunopathogenesis of virus diseases affecting the central nervous system. Crit. Rev. Immunol. **16:**145–222.
11. **Breder, C. D., M. Tsujimoto, Y. Terano, D. W. Scott, and C. B. Saper.** 1993. Distribution and characterization of tumor necrosis factor-alpha-like immunoreactivity in the murine central nervous system. J. Comp. Neurol. **337:** 543–567.
12. **Briese, T., M. Hornig, and W. I. Lipkin.** 1999. Bornavirus immunopathogenesis in rodents: models for human neurological diseases. J. Neurovirol. **5:**604–612.
13. **Carbone, K. M., S. W. Park, S. A. Rubin, I. I. Waltrip, and G. B. Vogelsang.** 1991. Borna disease: association with a maturation defect in the cellular immune response. J. Virol. **65:**6154–6164.
14. **Carbone, K. M., B. D. Trapp, J. W. Griffin, C. S. Duchala, and O. Narayan.** 1989. Astrocytes and Schwann cells are virus-host cells in the nervous system of rats with Borna disease. J. Neuropathol. Exp. Neurol. **48:**631–644.
15. **Caron, G., Y. Delneste, J. P. Aubry, G. Magistrelli, N. Herbault, A. Blaecke, A. Meager, J. Y. Bonnefoy, and P. Jeannin.** 1999. Human NK cells constitutively express membrane TNF-alpha (mTNFalpha) and present mTNFalpha-dependent cytotoxic activity. Eur. J. Immunol. **29:**3588–3595.
16. **Charles, P. C., X. Chen, M. S. Horwitz, and C. F. Brosnan.** 1999. Differential chemokine induction by the mouse adenovirus type-1 in the central nervous

system of susceptible and resistant strains of mice. J. Neurovirol. **5:**55–64.
17. **Cubitt, B., C. Oldstone, and J. C. de la Torre.** 1994. Sequence and genome organization of Borna disease virus. J. Virol. **68:**1382–1396.
18. **Davies, J. D., D. Mueller, D. B. Wilson, and D. P. Gold.** 1990. Nucleotide sequence of a cDNA encoding the rat T3 delta chain. Nucleic Acids Res. **18:**4617.
19. **De la Torre, J. C., and M. B. A. Oldstone.** 1996. Anatomy of viral persistence: mechanisms of persistence and associated disease. Adv. Virus Res. **46:**311–343.
20. **Deschl, U., L. Stitz, S. Herzog, K. Frese, and R. Rott.** 1990. Determination of immune cells and expression of major histocompatibility complex class II antigen in encephalitic lesions of experimental Borna disease. Acta Neuropathol. (Berlin) **81:**41–50.
21. **Dudov, K. P., and R. P. Perry.** 1984. The gene family encoding the mouse ribosomal protein L32 contains a uniquely expressed intron-containing gene and an unmutated processed gene. Cell **37:**457–468.
22. **Eddleston, M., and L. Mucke.** 1993. Molecular profile of reactive astrocytes—implications for their role in neurologic disease. Neuroscience **54:**15–36.
23. **Eisenman, L. M., R. Brothers, M. H. Tran, R. B. Kean, G. M. Dickson, B. Dietzschold, and D. C. Hooper.** 1999. Neonatal Borna disease virus infection in the rat causes a loss of Purkinje cells in the cerebellum. J. Neurovirol. **5:**181–189.
24. **Farber, J. M.** 1992. A collection of mRNA species that are inducible in the RAW 264.7 mouse macrophage cell line by gamma interferon and other agents. Mol. Cell. Biol. **12:**1535–1545.
25. **Farber, J. M.** 1997. Mig and IP-10: CXC chemokines that target lymphocytes. J. Leukoc. Biol. **61:**246–257.
26. **Fisher, S. N., P. Vanguri, H. S. Shin, and M. L. Shin.** 1995. Regulatory mechanisms of MuRantes and CRG-2 chemokine gene induction in central nervous system glial cells by virus. Brain Behav. Immun. **9:**331–344.
27. **Giulian, D.** 1993. Reactive glia as rivals in regulating neuronal survival. Glia **7:**102–110.
28. **Glabinski, A. R., and R. M. Ransohoff.** 1999. Chemokines and chemokine receptors in CNS pathology. J. Neurovirol. **5:**3–12.
29. **Gonzalez-Dunia, D., C. Sauder, and J. C. De la Torre.** 1997. Borna disease virus and the brain. Brain Res. Bull. **44:**647–664.
30. **Gosztonyi, G., and H. Ludwig.** 1995. Borna disease—neuropathology and pathogenesis. Curr. Top. Microbiol. Immunol. **190:**39–73.
31. **Guo, H., Y. X. Jin, M. Ishikawa, Y. M. Huang, P. H. van der Meide, H. Link, and B. G. Xiao.** 1998. Regulation of beta-chemokine mRNA expression in adult rat astrocytes by lipopolysaccharide, proinflammatory and immunoregulatory cytokines. Scand. J. Immunol. **48:**502–508.
32. **Hallensleben, W., L. Biro, C. Sauder, J. Hausmann, V. C. Asensio, I. L. Campbell, and P. Staeheli.** 2000. A polymorphism in the mouse Crg-2/IP-10 gene complicates chemokine gene expression analysis using a commercial ribonuclease protection assay. J. Immunol. Methods **234:**149–151.
33. **Hallensleben, W., M. Schwemmle, J. Hausmann, L. Stitz, B. Volk, A. Pagenstecher, and P. Staeheli.** 1998. Borna disease virus-induced neurological disorder in mice: infection of neonates results in immunopathology. J. Virol. **72:**4379–4386.
34. **Hatalski, C. G., W. F. Hickey, and W. I. Lipkin.** 1998. Evolution of the immune response in the central nervous system following infection with Borna disease virus. J. Neuroimmunol. **90:**137–142.
35. **Hausmann, J., W. Hallensleben, J. C. De la Torre, A. Pagenstecher, C. Zimmermann, H. Pircher, and P. Staeheli.** 1999. T cell ignorance in mice to Borna disease virus can be overcome by peripheral expression of the viral nucleoprotein. Proc. Natl. Acad. Sci. USA **96:**9769–9774.
36. **Hedrick, J. A., and A. Zlotnik.** 1997. Identification and characterization of a novel beta chemokine containing six conserved cysteines. J. Immunol. **159:**1589–1593.
37. **Herzog, S., and R. Rott.** 1980. Replication of Borna disease virus in cell cultures. Med. Microbiol. Immunol. **168:**153–158.
38. **Hesselgesser, J., and R. Horuk.** 1999. Chemokine and chemokine receptor expression in the central nervous system. J. Neurovirol. **5:**13–26.
39. **Hickey, W. F.** 1999. Leukocyte traffic in the central nervous system: the participants and their roles. Semin. Immunol. **11:**125–137.
40. **Hobbs, M. V., W. O. Weigle, D. J. Noonan, B. E. Torbett, R. J. McEvilly, R. J. Koch, G. J. Cardenas, and D. N. Ernst.** 1993. Patterns of cytokine gene expression by CD4+ T cells from young and old mice. J. Immunol. **150:**3602–3614.
41. **Hoffman, L. M., B. T. Fife, W. S. Begolka, S. D. Miller, and W. J. Karpus.** 1999. Central nervous system chemokine expression during Theiler's virus-induced demyelinating disease. J. Neurovirol. **5:**635–642.
42. **Hornig, M., H. Weissenböck, N. Horscroft, and W. I. Lipkin.** 1999. An infection-based model of neurodevelopmental damage. Proc. Natl. Acad. Sci. USA **96:**12102–12107.
43. **Hua, L. L., and S. C. Lee.** 2000. Distinct patterns of stimulus-inducible chemokine mRNA accumulation in human fetal astrocytes and microglia. Glia **30:**74–81.
44. **Klein, M. A., R. Frigg, E. Flechsig, A. J. Raeber, U. Kalinke, H. Bluethmann, F. Bootz, M. Suter, R. M. Zinkernagel, and A. Aguzzi.** 1997. A crucial role for B cells in neuroinvasive scrapie. Nature **390:**687–690.
45. **Kolb, S. A., B. Sporer, F. Lahrtz, U. Koedel, H. W. Pfister, and A. Fontana.** 1999. Identification of a T cell chemotactic factor in the cerebrospinal fluid of HIV-1-infected individuals as interferon-gamma inducible protein 10. J. Neuroimmunol. **93:**172–181.
46. **Kreutzberg, G. W.** 1996. Microglia: a sensor for pathological events in the CNS. Trends Neurosci. **19:**312–318.
47. **Kristensson, K., and E. Norrby.** 1986. Persistence of RNA viruses in the central nervous system. Annu. Rev. Microbiol. **40:**159–184.
48. **Kutsch, O., J. W. Oh, A. Nath, and E. N. Benveniste.** 1999. HIV-1 Tat induction of IL-8 and IP-10 by human primary astrocytes. Immunobiology **200:**694.
49. **Lahrtz, F., L. Piali, D. Nadal, H. W. Pfister, K. S. Spanaus, M. Baggiolini, and A. Fontana.** 1997. Chemotactic activity on mononuclear cells in the cerebrospinal fluid of patients with viral meningitis is mediated by interferon-gamma inducible protein-10 and monocyte chemotactic protein-1. Eur. J. Immunol. **27:**2484–2489.
50. **Lane, T. E., V. C. Asensio, N. Yu, A. D. Paoletti, I. L. Campbell, and M. J. Buchmeier.** 1998. Dynamic regulation of alpha- and beta-chemokine expression in the central nervous system during mouse hepatitis virus-induced demyelinating disease. J. Immunol. **160:**970–978.
51. **Legrand, C., M. Thomasset, C. O. Parkes, M. C. Clavel, and A. Rabie.** 1983. Calcium-binding protein in the developing rat cerebellum. An immunocytochemical study. Cell Tissue Res. **233:**389–402.
52. **Liang, P., L. Averboukh, W. Zhu, and A. B. Pardee.** 1994. Ras activation of genes: Mob-1 as a model. Proc. Natl. Acad. Sci. USA **91:**12515–12519.
53. **Lim, S. P., and A. Garzino-Demo.** 2000. The human immunodeficiency virus type 1 Tat protein up-regulates the promoter activity of the beta-chemokine monocyte chemoattractant protein 1 in the human astrocytoma cell line U-87 MG: role of SP-1, AP-1, and NF-κB consensus sites. J. Virol. **74:**1632–1640.
54. **Lin, R., C. Heylbroeck, P. Genin, P. M. Pitha, and J. Hiscott.** 1999. Essential role of interferon regulatory factor 3 in direct activation of RANTES chemokine transcription. Mol. Cell. Biol. **19:**959–966.
55. **Luster, A. D.** 1998. Chemokines—chemotactic cytokines that mediate inflammation. N. Engl. J. Med. **338:**436–445.
56. **Maciejewski-Lenoir, D., S. Chen, L. Feng, R. Maki, and K. B. Bacon.** 1999. Characterization of fractalkine in rat brain cells: migratory and activation signals for CX3CR-1-expressing microglia. J. Immunol. **163:**1628–1635.
57. **Morimoto, K., D. C. Hooper, A. Bornhorst, S. Corisedo, M. Bette, Z. F. Fu, M. K. Schäfer, H. Koprowski, E. Weihe, and B. Dietzschold.** 1996. Intrinsic responses to Borna disease infection of the central nervous system. Proc. Natl. Acad. Sci. USA **93:**13345–13350.
58. **Muller, U., U. Steinhoff, L. F. Reis, S. Hemmi, J. Pavlovic, R. M. Zinkernagel, and M. Aguet.** 1994. Functional role of type I and type II interferons in antiviral defense. Science **264:**1918–1921.
59. **Nazar, A. S., G. Cheng, H. S. Shin, P. N. Brothers, S. Dhib-Jalbut, M. L. Shin, and P. Vanguri.** 1997. Induction of IP-10 chemokine promoter by measles virus: comparison with interferon-gamma shows the use of the same response element but with differential DNA-protein binding profiles. J. Neuroimmunol. **77:**116–127.
60. **Neville, L. F., G. Mathiak, and O. Bagasra.** 1997. The immunobiology of interferon-gamma inducible protein 10 kD (IP-10): a novel, pleiotropic member of the C-X-C chemokine superfamily. Cytokine Growth Factor Rev. **8:**207–219.
61. **Oh, J. W., L. M. Schwiebert, and E. N. Benveniste.** 1999. Cytokine regulation of CC and CXC chemokine expression by human astrocytes. J. Neurovirol. **5:**82–94.
62. **Ohmori, Y., L. Wyner, S. Narumi, D. Armstrong, M. Stoler, and T. A. Hamilton.** 1993. Tumor necrosis factor-alpha induces cell type and tissue-specific expression of chemoattractant cytokines in vivo. Am. J. Pathol. **142:**861–870.
63. **Plata-Salaman, C. R., S. E. Ilyin, D. Gayle, A. Romanovitch, and K. M. Carbone.** 1999. Persistent Borna disease virus infection of neonatal rats causes brain regional changes of mRNAs for cytokines, cytokine receptor components and neuropeptides. Brain Res. Bull. **49:**441–451.
64. **Ransohoff, R. M., A. Glabinski, and M. Tani.** 1996. Chemokines in immune-mediated inflammation of the central nervous system. Cytokine Growth Factor Rev. **7:**35–46.
65. **Rollins, B. J.** 1997. Chemokines. Blood **90:**909–928.
66. **Rott, R., and H. Becht.** 1995. Natural and experimental Borna disease in animals. Curr. Top. Microbiol. Immunol. **190:**17–30.
67. **Sanders, V. J., C. A. Pittman, M. G. White, G. Wang, C. A. Wiley, and C. L. Achim.** 1998. Chemokines and receptors in HIV encephalitis. AIDS **12:**1021–1026.
68. **Sasseville, V. G., M. M. Smith, C. R. Mackay, D. R. Pauley, K. G. Mansfield, D. J. Ringler, and A. A. Lackner.** 1996. Chemokine expression in simian immunodeficiency virus-induced AIDS encephalitis. Am. J. Pathol. **149:**1459–1467.
69. **Sauder, C., and J. C. De la Torre.** 1999. Cytokine expression in the rat central nervous system following perinatal Borna disease virus infection. J. Neuroimmunol. **96:**29–45.
70. **Schmidtmayerova, H., H. S. Nottet, G. Nuovo, T. Raabe, C. R. Flanagan, L.**

Dubrovsky, H. E. Gendelman, A. Cerami, M. Bukrinsky, and B. Sherry. 1996. Human immunodeficiency virus type 1 infection alters chemokine beta peptide expression in human monocytes: implications for recruitment of leukocytes into brain and lymph nodes. Proc. Natl. Acad. Sci. USA **93:**700–704.

71. **Shankar, V., M. Kao, A. N. Hamir, H. Sheng, H. Koprowski, and B. Dietzschold.** 1992. Kinetics of virus spread and changes in levels of several cytokine mRNAs in the brain after intranasal infection of rats with Borna disease virus. J. Virol. **66:**992–998.
72. **Simmons, D. M., J. L. Arriza, and L. W. Swanson.** 1989. A complete protocol for in situ hybridization of messenger RNAs in brain and other tissues with radiolabeled single-stranded RNA probes. J. Histotechnol. **12:**169–181.
73. **Stitz, L., B. Dietzschold, and K. M. Carbone.** 1995. Immunopathogenesis of Borna disease. Curr. Top. Microbiol. Immunol. **190:**75–92.
74. **van den Elsen, P., K. Georgopoulos, B. A. Shepley, S. Orkin, and C. Terhorst.** 1986. Exon/intron organization of the genes coding for the delta chains of the human and murine T-cell receptor/T3 complex. Proc. Natl. Acad. Sci. USA **83:**2944–2948.
75. **Vanguri, P., and J. M. Farber.** 1990. Identification of CRG-2. An interferon-inducible mRNA predicted to encode a murine monokine. J. Biol. Chem. **265:**15049–15057.
76. **Vanguri, P., and J. M. Farber.** 1994. IFN and virus-inducible expression of an immediate early gene, crg-2/IP-10, and a delayed gene, I-A alpha, in astrocytes and microglia. J. Immunol. **152:**1411–1418.
77. **Wang, X., T. L. Yue, E. H. Ohlstein, C. P. Sung, and G. Z. Feuerstein.** 1996. Interferon-inducible protein-10 involves vascular smooth muscle cell migration, proliferation, and inflammatory response. J. Biol. Chem. **271:**24286–24293.
78. **Williams, A. F., G. Galfre, and C. Milstein.** 1977. Analysis of cell surfaces by xenogeneic myeloma-hybrid antibodies: differentiation antigens of rat lymphocytes. Cell **12:**663–673.
79. **Yoshimura, T., M. Takeya, and K. Takahashi.** 1991. Molecular cloning of rat monocyte chemoattractant protein-1 (MCP-1) and its expression in rat spleen cells and tumor cell lines. Biochem. Biophys. Res. Commun. **174:**504–509.
80. **Zocher, M., S. Czub, J. Schulte-Mönting, J. C. de la Torre, and C. Sauder.** Alterations in neurotrophin and neurotrophin receptor gene expression patterns in the rat central nervous system following perinatal Borna disease virus infection. J. Neurovirol., in press.